HHS Public Access
Author manuscript

Immunity. Author manuscript; available in PMC 2017 February 16.

CD45 Phosphatase Inhibits STAT3 Transcription Factor Activity in Myeloid Cells and Promotes Tumor-Associated Macrophage Differentiation

Vinit Kumar[1], **Pingyan Cheng**[2], **Thomas Condamine**[1], **Sridevi Mony**[1], **Lucia R. Languino**[3], **Judith C. McCaffrey**[2], **Neil Hockstein**[4], **Michael Guarino**[4], **Gregory Masters**[4], **Emily Penman**[4], **Fred Denstman**[4], **Xiaowei Xu**[5], **Dario C. Altieri**[1], **Hong Du**[6], **Cong Yan**[6], and **Dmitry I. Gabrilovich**[1,*]

[1]The Wistar Institute, Philadelphia, PA 19104, USA

[2]H. Lee Moffitt Cancer Center, Tampa, FL 33612, USA

[3]Thomas Jefferson University, Philadelphia, PA 19110, USA

[4]Helen F. Graham Cancer Center & Research Institute, Christiana Care Health System, Newark, DE 19713, USA

[5]University of Pennsylvania, Philadelphia, PA 19104, USA

[6]Indiana University School of Medicine, Indianapolis, IN 46202, USA
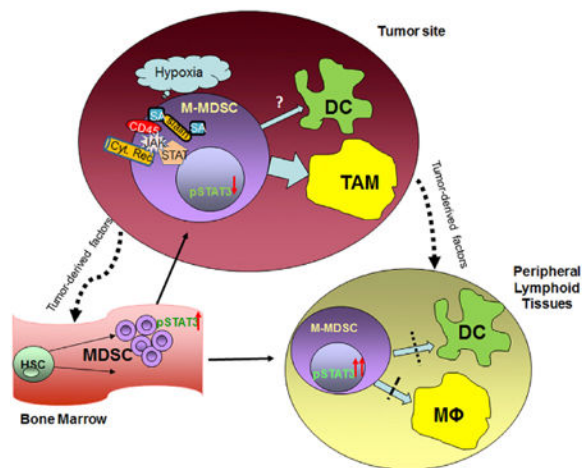
Summary

Recruitment of monocytic myeloid-derived suppressor cells (MDSCs) and differentiation of tumor-associated macrophages (TAMs) are the major factors contributing to tumor progression and metastasis. We demonstrated that differentiation of TAMs in tumor site from monocytic precursors was controlled by downregulation of the activity of the transcription factor STAT3. Decreased STAT3 activity was caused by hypoxia and affected all myeloid cells but was not observed in tumor cells. Upregulation of CD45 tyrosine phosphatase activity in MDSCs exposed to hypoxia in tumor site was responsible for downregulation of STAT3. This effect was mediated by the disruption of CD45 protein dimerization regulated by sialic acid. Thus, STAT3 has a unique function in the tumor environment in controlling the differentiation of MDSC into TAM, and its regulatory pathway could be a potential target for therapy.

Graphical abstract

*Correspondence: dgabrilovich@wistar.org.

Introduction

The critical role of myeloid cells in regulating tumor growth and metastases is well established (Galdiero et al., 2013). Substantial expansion of myeloid-derived suppressor cells (MDSCs) is one of the important clinically relevant features of cancer. MDSCs are immature, pathologically activated myeloid cells, which are phenotypically and morphologically similar to monocytes (Mono)—M-MDSC and polymorphonuclear neutrophils (PMNs)—PMN-MDSC, but distinct in functional and biochemical characteristics and the ability to suppress immune responses (Gabrilovich and Nagaraj, 2009). Under physiological conditions, myeloid cells in tissues are comprised primarily of terminally differentiated macrophages, dendritic cells (DCs), and PMNs as well as relatively small population of Mon. Under steady state conditions, with some exceptions, tissues macrophages proliferate locally with only small proportion of macrophages derived from circulating Mon (Bain et al., 2014; Schulz et al., 2012). In lymphoid organs of tumor-bearing (TB) hosts, MDSCs have inefficient differentiation to macrophages and DC. However, after migration to a tumor site, M-MDSC rapidly differentiate to tumor-associated macrophages (TAMs) (Gabrilovich et al., 2012; Solito et al., 2010) and recent data indicate that circulating Mon or M-MDSC are essential for TAM accumulation (Franklin et al., 2014; Noy and Pollard, 2014) (Shand et al., 2014).

One of the major factors that drives MDSC expansion in cancer is transcriptional factor signal transducer and activator of transcription 3 (STAT3) (Gabrilovich et al., 2012). Ablation of STAT3 expression through the use of conditional knockout mice or selective STAT3 inhibitor markedly reduced the expansion of MDSC and increased T cell responses in tumor-bearing mice (Kortylewski et al., 2005; Nefedova et al., 2005b). STAT3 is critically important for cell proliferation, survival, and motility (Stark and Darnell, 2012). It is activated by phosphorylation at C-terminal Tyr 705 by Janus-activated kinases (JAK); or Ser 727 by protein kinase C, mitogen-activated protein kinases, and CDK5; and by reversible acetylation by histone acetyltransferase on Lys 685. Following activation, STAT3 undergoes homodimerization and nuclear translocation where it regulates gene expression. Targeting of STAT3 in myeloid cells is considered as an attractive therapeutic opportunity,

based on the assumption that STAT3 activity in tumor myeloid cells remains high, especially given the fact that many tumor cells have high STAT3 (Kortylewski et al., 2005). However, STAT3 targeting had only limited clinical success (Yu et al., 2014). Inhibition of STAT3 was found to reduce MDSC accumulation only in the spleens, but not in the tumors (Ko et al., 2010). It was reported that deletion of STAT3 in the myeloid compartment actually increased the percentage of M-MDSC (Abad et al., 2014) (Tu et al., 2012) in tumors and did not affect the tumor incidence in these mice (Abad et al., 2014). This suggests a complex and not yet appreciated role of STAT3 in myeloid cells in tumors.

Here, we report profound downregulation of STAT3 activity in MDSCs in tumors as compared to the same cells in peripheral lymphoid organs and blood. This decrease was a critical factor in the regulation of MDSC differentiation to TAM. We found that downregulation of STAT3 activity was caused by hypoxia. However, it was independent of HIF-1α but instead was controlled by CD45 protein tyrosine phosphatases (PTP). Inhibition of CD45PTP sensitized myeloid cells in tumor site to the selective STAT3 inhibitor. Thus, tumor hypoxia caused activation of CD45 PTP that resulted in downregulation of STAT3 activity and promoted M-MDSC differentiation to tumor-promoting TAM.

Results

STAT3 Activity in Tumor MDSC

We evaluated myeloid cells in mice bearing two transplantable tumors (EL4 lymphoma, CT26 colon carcinoma) and two transgenic tumors (Ret melanoma and TRAMP prostate carcinoma). Expression of the human *ret* oncogene in melanocytes resulted in spontaneous development of metastatic melanomas (Kato et al., 1998; Meyer et al., 2011). In the TRAMP model SV40 large T and small t oncogenes are expressed in the prostatic epithelium under the control of the minimal rat probasin promoter resulting in the appearance of prostatic intraepithelial neoplasia, invasive cancer, and metastasis (Kaplan-Lefko et al., 2003). In all four models, the vast majority of CD11b$^+$ myeloid cells in spleens were represented by Gr-1$^+$ MDSCs. In contrast, in tumors the majority of myeloid cells were represented by Gr-1$^-$F4/80$^+$ macrophages and CD11c$^+$IA^{b+} DC (Figure S1A).

To assess the composition of myeloid cells in cancer patients, we gated total population of CD45$^+$CD33$^+$ myeloid cells in peripheral blood and tumor tissues obtained from patients with surgically resectable colon, breast, or non-small lung cancers. We focused on Mon and M-MDSC because macrophages are not present in peripheral blood. In all three types of cancer the proportion of CD11b$^+$CD14$^+$HLA-DR$^{-/lo}$ M-MDSC among myeloid cells was dramatically lower in tumor tissues than in peripheral blood (Figure S1B).

Pharmacological inhibition of STAT3 is known to reduce MDSC presence in spleens of TB mice (Herrmann et al., 2010; Nefedova et al., 2005b; Xin et al., 2009). We investigated whether selective STAT3 inhibitor cucurbitacin I (JSI-124) (Blaskovich et al., 2003; Nefedova et al., 2005a) would target tumor MDSC. EL-4 tumor cells were not sensitive to JSI-124 in vitro (data not shown) and their growth was not affected by JSI-124 in vivo (Figure 1A). JSI-124 significantly decreased the presence of PMN-MDSC, M-MDSC, and

slightly decreased macrophages in spleens of TB mice. The proportion of DC was increased (Figure 1B). However, JSI-124 did not affect myeloid cells in tumors (Figure 1C).

These results raised the questions of whether STAT3 activity in spleen and tumor MDSC was different. To address this question, we isolated total populations of $CD11b^+Gr-1^+F4/80^-$ MDSC from tumors (ascites) and spleens of the same EL-4 TB mice (Figure S1C). MDSC in tumors had sharply lower STAT3 activity than cells in spleen as was measured by the level of tyrosine phosphorylation (Figure 1D) and DNA binding (Figure 1E). To verify these observations in different models, we tested pSTAT3 expression by flow cytometry in MDSC from mice bearing EL-4, CT26, 4T1 mammary adenocarcinoma, and B16F10 melanoma, as well as Ret melanoma and TRAMP prostate cancer. Both tumor tissues and spleens underwent enzymatic digestion. In all tested models MDSC in spleens had significantly higher pSTAT3 than the cells with the same phenotype in tumor site (Figure 1F). Similar differences in pSTAT3 were observed in macrophages (Figure 1G). The decrease in pSTAT3 expression was seen in both populations of MDSC in tumor site (Figure S1D). As expected, tumor M-MDSC had potent immune suppressive activity (Figure S1E).

The Fate of M-MDSC in Tumor-Bearing Mice Is Linked with STAT3 Activity

To confirm these observations, we traced the fate of M-MDSC after adoptive transfer. $CD11b^+Ly6C^{hi}Ly6G^-F4/80^-$ M-MDSC sorted from BM of EL-4 TB mice were labeled with fluorescent dye DDAO and injected intravenously (i.v.) to EL-4 TB recipient. 48 hr later, the phenotype of donor's populations was evaluated (Figure 2A). In spleens, 60% of donor's cells retained the phenotype of M-MDSC with only 20% of cells acquired the phenotype of macrophages ($CD11b^+Ly6G^-F4/80^+IAb^+$). In tumors of the same mice, M-MDSC population represented less than 20% of donor's cells with 60% of the cells being macrophages (Figures 2A and 2B). Most of the TAMs expressed CD206 (Figure 2A). The expression of pSTAT3 in M-MDSC and macrophages from tumors was significantly lower than in cells from spleen of the same mice (Figure 2C).

Using samples from patients with head and neck cancer (Figure 2D) we found that MDSC in tumor site had significantly lower pSTAT3 than MDSC in peripheral blood (Figure 2E). To verify these observations, we evaluated fixed tumor tissues and tumor-free lymph nodes collected from patients with melanoma. The intensity of pSTAT3 fluorescence was measured in nuclei of CD33 positive myeloid cells (Figure 2F). Myeloid cells in tumor tissues had significantly lower pSTAT3 than $CD33^+$ cells in lymph nodes (Figure 2G).

STAT3 Activity Regulates M-MDSC Differentiation

Thus, after migration to tumor site, STAT3 activity in M-MDSC was substantially inhibited. We asked whether this inhibition has an impact on the fate of these cells. To address this question, we used mice with constitutively active STAT3: FVB/n STAT3C mice with doxycycline-inducible STAT3 activation targeted to myeloid cells (c-fms-rtTA/(TetO)$_7$-CMV-Stat3C) (Yan et al., 2012). To target STAT3 activation only to recent BM derived myeloid cells, we reconstituted lethally irradiated FVB/n recipients with BM from STAT3C mice. Donor's and recipient mice not receiving doxycycline served as a control. Another

control included wild-type (WT) mice reconstituted with WT BM and treated with doxycycline. As expected, constitutive activation of STAT3 resulted in expansion of Gr-1$^+$CD11b$^+$ myeloid cells in spleens of naive recipients (Figure S2A). Eight weeks after BM transfer, mice were injected subcutaneously (s.c.) with syngeneic ANV mammary carcinoma tumor cells. BM M-MDSC were sorted 3 weeks later and transferred to syngeneic ANV TB mice. WT M-MDSC rapidly differentiated to macrophages in tumors but not in spleen. In contrast, STAT3C M-MDSC differentiated to macrophages equally in spleens and tumors (Figure 3A).

In parallel experiments, 8 weeks after BM transfer, mice were injected s.c. with ANV tumor cells and 3 weeks later myeloid cells were evaluated directly in spleens and tumors of recipient mice. No differences were observed in the presence of tumor CD11b$^+$ cells between recipients of WT and STAT3C BM (data not shown). TAM represented the predominant population of myeloid cells in tumors of control mice outnumbering MDSC by 4:1 ratio (Figure 3B). In contrast, in tumors of mice with STAT3C BM, the proportion of MDSC and TAM were similar. The proportion of TAM in recipients of STAT3C BM was significantly lower and MDSC significantly higher than in both control groups of mice (Figure 3B) including both M-MDSC and PMN-MDSC populations (Figure 3C). In spleens, all populations of MDSC were not affected by STAT3 activation (Figures 3B and 3C). However, these changes did not affect tumor growth in these mice (Figure 3D). We hypothesized that upregulation of PMN-MDSC in these mice compensated for the decrease in TAM. To test this possibility, we used Gr-1 antibody that depletes MDSC in spleen and blood (Figure S2B). Treatment with Gr-1 antibody caused profound depletion of PMN-MDSC in tumors but had little effect on M-MDSC and TAM (Figure 3E) and did not affect tumor growth (Figure 3F). Combination of MDSC depletion and STAT3 activation in myeloid cells significantly reduced tumor growth (Figure 3F). These data support the important role of STAT3 in regulation of TAM differentiation and provide additional impetus to the concept that PMN-MDSC and mononuclear myeloid cells contribute to tumor progression and can compensate for each other loss.

Hypoxia Inhibits STAT3 Activity in MDSC

Hypoxia is a critical element of the tumor microenvironment. Previous studies have implicated hypoxia in the immune suppressive activity of TAM and MDSC (Corzo et al., 2010; Doedens et al., 2010). We tested the effect of hypoxia on STAT3 activity in total MDSC isolated from spleens of TB mice. To better mimic conditions present in tumor site in all in vitro experiments, MDSCs were cultured with 20 ng/ml GM-CSF and 20% tumor explant supernatants (TES). Hypoxia caused dramatic downregulation of STAT3 DNA binding activity (Figure 4A) and the amount of pSTAT3 (Figure 4B). Similar results were obtained in the population of highly purified M-MDSC (Figure 4C). To evaluate the relevance of these findings in vivo, we injected CT26 TB mice i.v. with hypoxyprobe - pimonidazole HCl and tumors were collected 1 hr later. pSTAT3 was measured in total MDSC with a different level of hypoxia (Figure 4D). MDSC in a more hypoxic environment had significantly lower level of pSTAT3 than MDSC in a less hypoxic environment (Figure 4E). We verified these observations in a separate experiment where populations of M-MDSC and PMN-MDSC were evaluated (Figure 4F).

To test the effect of hypoxia in humans, we cultured PBMC from peripheral blood of patients with NSCLC and head and neck cancer (HNC) for 48 hr in hypoxia in the presence of GM-CSF and tumor cell conditioned medium. pSTAT3 was measured in $CD11b^+CD14^-CD33b^+$ MDSC. We found a significant decrease in the expression of pSTAT3 in MDSC caused by hypoxia (Figure 4G). In contrast to the data obtained in myeloid cells, hypoxia not only did not decrease pSTAT3 in tumor cells, but in many cells also caused substantial upregulation of pSTAT3 (Figure 4H).

Hypoxia Induced Upregulation of CD45 Phosphatase in Myeloid Cells

What could be the mechanism of selective inhibition of STAT3 in myeloid cells? STAT1 and STAT3 often have antagonistic effects on cell functions (Shim et al., 2009). In our experiments, hypoxia caused modest upregulation of pSTAT1 in MDSC (Figure S3A). However, hypoxia caused similar downregulation of pSTAT3 in STAT1-deficient and WT MDSC (Figure S3B). HIF-1α is a critical factor regulating the cellular response to hypoxia. To assess its effect on STAT3 activity, we reconstituted lethally irradiated recipient mice with BM from WT and HIF-1α-deficient ($Hif1a^{-/-}$) mice and established EL4 tumors in these mice intraperitoneally (i.p.) $Hif1a^{-/-}$ tumor MDSC had the same level of pSTAT3 as WT MDSC (Figure S3C). Exposure of spleen MDSC from TB WT and $Hif1a^{-/-}$ mice to hypoxia caused an equal decrease in pSTAT3 (Figure 4D). These results indicated that STAT1 or HIF-1α was not involved in regulation of STAT3 activity by hypoxia.

STAT3 activation could be negatively regulated by the protein inhibitor of activated STAT (PIAS), which affects STAT transcriptional activity by blocking DNA binding; by suppressors of cytokine signaling (SOCS), which prevents JAK from activating STAT3; and by protein tyrosine phosphatases (PTEN, CD45, SHP-1, SHP-2), which remove phosphates from activated STATs (Rébé et al., 2013). CD45PTP is present in hematopoietic cells but not in epithelial tumor cells and was implicated in dephosphorylation of Src family kinases and downregulation pSTAT3 (Holmes, 2006; Wu et al., 2009). We hypothesized that CD45PTP could be involved in regulation of STAT3 activity in myeloid cells. We found no difference in the expression of CD45 between MDSC from tumor site and spleen as well as no effect of hypoxia on CD45 expression in MDSC (data not shown). However, when phosphatase activity of CD45PTP was measured, $Gr-1^+CD11b^+$ MDSC from tumors in two different models displayed a significantly higher activity than MDSC from spleen (Figure 5A). Significantly higher CD45PTP activity was found in tumor M-MDSC and PMN-MDSC than in their counterparts in spleens (Figure 5B). Exposure of splenic M-MDSC and PMN-MDSC to hypoxia resulted in a significant increase in CD45PTP activity (Figure 5C). Increased CD45PTP activity was also found in MDSC isolated from the peripheral blood of patients with HNC and exposed to hypoxia (Figure 5D). These results indicate that hypoxia directly causes upregulation of CD45PTP in myeloid cells.

To evaluate the possible involvement of CD45 PTP in the regulation of pSTAT3, we used several experimental approaches. CD45 expression was downregulated in spleen MDSC using siRNA (Figure S4A). This inhibition of CD45 expression abrogated the downregulation of pSTAT3 in MDSC caused by hypoxia (Figure S4B). We also used BM cells from CD45-deficient ($Ptprc^{-/-}$) mice (Xu and Weiss, 2002) (Figures 5E and 5F). HPC

from WT and *Ptprc*$^{−/−}$ mice were cultured for 6 days with GM-CSF and TES. Gr-1$^+$CD11b$^+$ cells were then purified and exposed to hypoxia. In contrast to WT MDSC, in CD45 deficient MDSC hypoxia did not cause a decrease in pSTAT3 (Figure 5G). Cells generated from CD45 deficient HPC had a substantially higher expression of pSTAT3 than cells generated from WT HPC (Figure 5H).

To assess the effect of the tumor microenvironment on the fate of MDSC, HPC from CD45 WT or *Ptprc*$^{−/−}$ mice were cultured with GM-CSF and TES for 6 days, MDSC were purified, and WT and CD45 deficient MDSC were labeled with two fluorescent cell trackers CMFDA and DDAO, mixed at 1:1 ratio, and injected into the ascites of EL-4 TB mice. Two days later, cells from ascites were collected and cells positive for CMFDA or DDAO were evaluated. Among CD11b$^+$Gr-1$^+$ cells *Ptprc*$^{−/−}$ cells were predominant, outnumbering CD45WT cells by 3:1 ratio, whereas among CD11b$^+$F4/80$^+$Gr-1$^−$ macrophages CD45 WT cells outnumbered *Ptprc*$^{−/−}$ cells by 4:1 (Figure 5I).

We studied whether lack of CD45 affected the differentiation of myeloid cells from HPC. In the absence of TES, no differences in the proportion of macrophages and Gr-1$^+$CD11b$^+$ cells were found between WT and *Ptprc*$^{−/−}$ cells (Figure 5J). However, when the same experiment was performed in the presence of TES, the proportion of CD11b$^+$Gr-1$^+$ cells generated from CD45 deficient HPC was significantly higher and the proportion of macrophages was significantly lower than in cells generated from WT HPC (Figure 5J). This effect is likely due to the fact that TES caused a significant increase in pSTAT3 in myeloid cells (Figure 5K).

If hypoxia via CD45PTP regulates pSTAT3 in MDSC, then why similar changes in pSTAT3 were not observed in EL-4 cells also expressing CD45? When compared with spleen MDSC, EL-4 cells had very low level of pSTAT3 (Figure S5A). CD45 activity in EL4 cells was almost 3-fold higher than in MDSC (Figure S5B) and hypoxia did not change its activity (Figure S5C). Thus, high basal expression of CD45 activity in EL4 cells may explain relatively low basal level pSTAT3 and lack the effect of hypoxia.

The Mechanism of CD45 Activation in Hypoxia

Several isoforms of CD45 have been described (Holmes, 2006). Although the data on functional disparity between different isoforms are not conclusive, it has been suggested that the CD45RA isoform has a more potent PTP activity than the CD45RO isoform. In our experiments, hypoxia did not change the expression of CD45RA in MDSC (Figure 6A). We tested the possibility that different galectins, known to be produced under hypoxic conditions, trigger CD45 PTP activity and de-phosphorylation of STAT3. However, treatment of MDSC with Gal-1 or Gal-3 did not affect pSTAT3 (data not shown).

Dimerization of CD45 can play a major role in the regulation of its activity (Xu and Weiss, 2002). The monomeric form of CD45 is more active than the dimer form. We evaluated the effect of hypoxia on the formation of CD45 dimers in MDSC. Dimer was a prevalent form of CD45 in MDSC in normoxia. Hypoxia caused a dramatic shift from dimer to monomeric form of CD45 (Figure 6B).

Dimerization of CD45 is largely modulated by sialylation (Xu and Weiss, 2002). To test the hypothesis that binding of sialic acid (SA) to CD45 is regulated in tumor microenvironment, we incubated lysates of MDSC from spleen and tumors of EL4 TB mice with agarose-bound Sambucus Nigra Bark Lectin (SNA) and probed with CD45 antibody or Siglec E antibody to verify loading control. MDSC from tumor site but not from spleen had high amount of SA bound CD45 (Figure 6C). The presence of SA on the surface of MDSC was evaluated by using two different lectins: maackia amurensis lectin II recognizing α-2,3 linked sialic acid and SNA recognizing α-2,6 linked sialic acid. Both lectins demonstrated substantially higher binding to the surface of MDSC from tumors than spleens (Figure 6D).

Sialin is a major SA transporter and its expression has been shown to be upregulated during hypoxia in human cancer cells (Yin et al., 2006). We found that hypoxia induced substantial upregulation of sialin in mouse (Figure 6E) and human (Figure 6F) MDSC and MDSC isolated from tumors had a substantially higher amount of sialin than MDSC from spleens (Figure 6G). Incidentally, EL4 tumor cells had substantially higher level of sialin than MDSC and that level was not changed in hypoxia (Figure S5D). These results suggest increased level of sialin in these cells could contribute to increased SA transport to cell surface and increased basal CD45PTP activity in EL4 cells.

We tested the functional consequences of hydrolytic degradation of sialic acid in MDSC using sialidase (neuraminidase). Sialidase treatment completely abrogated CD45PTP activity (Figure 6H) and downregulation of pSTAT3 in MDSC exposed to hypoxia. However, sialidase had no effect of pSTAT3 levels in MDSC in normoxia (Figure 6I). Hypoxia decreased population of immature Gr-1$^+$CD11b$^+$ cells and, specifically, CD11b$^+$ Ly6C^{high}Ly6G$^-$ Mon and promoted differentiation of macrophages from HPC in vitro. The presence of sialidase abrogated this effect (Figure 6J). The presence of CD11b$^+$Ly6C^{low}Ly6G$^+$ granulocytic cells was not affected by hypoxia and sialidase (Figure 6J). Differentiation of HPC from STAT3C mice was heavily skewed toward Gr-1$^+$CD11b$^+$ cells. Hypoxia did not affect macrophages differentiation and no effect of sialidase was observed (Figure 6K). These data support the concept of regulation of myeloid cell differentiation in hypoxia by CD45PTP activated by SA.

Sialidase Sensitizes Myeloid Cells to STAT3 Inhibitors

We tested the possible effect of sialidase in vivo in combination with STAT3 inhibitor JSI-124. We used MethA sarcoma, which is resistant to STAT3 inhibitors (Nefedova et al., 2005b). Combination of sialidase with JSI-124 did not affect the viability of these cells in vitro, in contrast to sensitive CT26 tumor cells (Figure S6). MethA sarcoma was established s.c. in BALB/c mice and on day 7 when tumors became palpable, mice were treated with JSI-124 (1mg/kg i.p. daily for 6 days per week for 3 weeks) alone or in combination with sialidase (intratumoral administration, twice a week, 200 mU/mouse for 3 weeks). Consistent with observation in EL-4 tumor model (Figure 1), JSI-124 alone did not affect tumor growth. Treatment with sialidase alone enhanced tumor progression (Figure 7A). Sialidase treatment caused upregulation of pSTAT3 in tumor MDSC (Figure 7B) and increase in the presence of CD45$^+$CD11b$^+$ myeloid cells in tumor site (Figure 7C). Population of tumor MDSC was significantly higher and TAM significantly lower than in

control mice. However, sialidase treatment alone did not affect populations of myeloid cells in spleens (Figure 7D), which supported the specific nature of its effect on STAT3 in tumors. Treatment of mice with JSI-124 alone did not affect tumor growth (Figure 7A) and the presence of myeloid cells in tumor site (Figures 7C and 7D). However, similar to the results observed in other models, it significantly decreased MDSC in spleens (Figure 7D). In sharp contrast, the combination of sialiadase and JSI-124 resulted in substantial antitumor effect (Figure 7A). In most of mice tumors were not detectable after 4 weeks of treatment. Myeloid cells were practically undetectable in tumors during the treatment (Figure 7D and data not shown). These results suggested that sialidase could sensitize tumor myeloid cells to STAT3 inhibition and dramatically enhance the antitumor effect of STAT3 targeted therapy. Because the antitumor effect of combination treatment was strong, it was unclear whether this combination truly affected myeloid cells. To address this question, we started treatment in separate experiments after tumors reached 1 cm in diameter. Even in such big tumors, combination therapy caused antitumor effect (Figure 7E). To assess early changes in myeloid cells, we terminated the experiment as soon as the differences in tumor size became evident (10 days after start of the treatment). The combination of sialidase with JSI-124 caused significant decrease in the presence of myeloid cells in tumors (Figure 7F). Changes in populations of myeloid cells in spleens were very similar to those observed in mice treated at early stages of tumor development (Figure 7G). In tumors, combination of JSI-124 with sialidase caused significant decrease in the population of MDSC but did not affected macrophages (Figure 7G). These data indicate that decrease in MDSC in tumor site induced by combination therapy precedes substantial changes in tumor size.

Discussion

Here, we report that tumor MDSCs have dramatically lower STAT3 activity than their counterparts in spleen of mice or blood of cancer patients and this downregulation was consequential for M-MDSC ability to differentiate to TAM. These observations were rather surprising since STAT3 upregulation was widely reported for myeloid cells in TB hosts. STAT3 is one of the major drivers of MDSC expansion and is involved in MDSC mediated immune suppression (Nefedova et al., 2004; Rébé et al., 2013; Trikha and Carson, 2014). However, most of the data describing STAT3 activity in myeloid cells in cancer were obtained either in vitro or in cells isolated from peripheral lymphoid organs (Bharadwaj et al., 2007; Hasita et al., 2010; Park et al., 2004; Sun et al., 2006). In glioblastoma, TAM were shown to be predominantly STAT3-positive (Komohara et al., 2008). However, the level of STAT3 was not compared between TAM and peripheral macrophages. Several studies reported effect of STAT3 ablation in myeloid cells on antitumor activity as well as on angiogenesis (Kortylewski et al., 2005; Kujawski et al., 2008). However, the direct assessments of the level of STAT3 activity between tumor MDSC and spleen MDSC with the same phenotype were not performed. In a recent study it was reported that the proportion of CD14+HLA-DR[lo] MDSC in tumors of patients with HNC was higher than in peripheral blood and that those tumor associated cells had a higher level of pSTAT3 than the cells in peripheral blood (Vasquez-Dunddel et al., 2013). However, in that study only the proportion of pSTAT3-positive cells was evaluated. Most myeloid cells are positive for pSTAT3 and in our hands the calculation of the proportion of the cells was not informative. When we

compared in the same experiment the intensity of pSTAT3 fluorescence in tumor and blood MDSC from the same patient, we observed a significant decrease in pSTAT3 expression in tumor MDSC.

Constitutive activation of STAT3 in myeloid cells promoted accumulation of Gr-1$^+$CD11b$^+$ in spleen, which is consistent with the known role of STAT3 in myelopoiesis. In ANV TB mice, expansion of MDSC in spleen was so prominent that additional activation of STAT3 did not affect their accumulation in spleen and BM. This provided us with the opportunity to assess potential direct contribution of STAT3 in myeloid cell fate in tumors. In TB mice that received transfer of control BM, TAM were predominant population of myeloid cells. In contrast, in tumors of mice with STAT3C BM, MDSC represented the largest population. Since the total number of myeloid cells inside tumors was not different, one possible explanation was that in STAT3C mice MDSC migrated much more to the tumor site and thus decreased the proportion of TAM. The number of MDSC subsets in spleens and BM of TB WT and STAT3C mice was the same. Although different migration pattern in STAT3C MDSC is possible, we approached this question from different side by depleting MDSC using Gr-1 antibody. If increased recruitment of MDSC was the main mechanism of observed decrease in TAM presence in STAT3C mice, then short-time depletion of MDSC in blood and spleen should result in decreased proportion M-MDSC and thus increase the proportion of TAM. However, Gr-1 antibody depleted only PMN-MDSC in tumors and did not affect M-MDSC or TAM. Importantly, potent antitumor effect was observed only when the combination of blocked TAM differentiation, due to STAT3C overexpression, with depletion of PMN-MDSC was used. This supports the concept that different populations of myeloid cells contribute to tumor progression and inhibition or elimination of only one of them may not be sufficient to obtain antitumor effect.

In this study, we focused on the molecular mechanisms that regulate STAT3 in tumor myeloid cells. Our experiments demonstrated that downregulation of STAT3 activity in MDSC was caused by hypoxia and mediated via activation of CD45PTP specific for hematopoietic cells. In the absence of CD45 on myeloid cells, the tumor microenvironment and hypoxia failed to downregulate pSTAT3 in these cells and prevented rapid differentiation of M-MDSC to TAM. We found that hypoxia disrupted CD45 dimerization, which is known to regulate CD45PTP activity (Xu and Weiss, 2002). Our data demonstrated that in tumors and in hypoxic conditions MDSC upregulated sialin, a SA transporter. This facilitated the transport of sialic acid to the cell surface and its direct binding to CD45 leading to the disruption of CD45 dimerization. Experiments in vivo further support this mechanism. Intratumoral administration of sialidase promoted tumor progression. Activation of STAT3 in tumor myeloid cells could be one of the mechanisms of this effect. It is likely that other effect of sialidase on tumor stroma and/or angiogenesis could also contribute to this phenomenon. However, the fact that combination of sialidase with STAT3 inhibitor had profound antitumor effect associated with depletion of myeloid cells in tumor site argues in support of the role of sialidase in regulation of STAT3 activity.

Thus, we present a novel model of regulation of the fate of myeloid cells in TB hosts mediated by STAT3. The expansion of MDSC in cancer is controlled by STAT3 activation. It promotes cell proliferation and prevents differentiation of M-MDSC to macrophages and

DC. When M-MDSC migrate to the tumor site, hypoxia, via upregulation of SA transport and its binding to CD45, increases the CD45 PTP activity in these cells, which leads to a rapid de-phosphorylation of STAT3 and downregulation of its activity. This facilitates MDSC differentiation to TAM. These new mechanisms might have an implication for the design of new targeted therapy.

Experimental Procedures

Human Subjects and Samples

Studies were approved by the Institutional Review Boards of the University of South Florida, Helen F. Graham Cancer Center, and The Wistar Institute. The patient samples were collected with informed consent. Peripheral blood (PB) and tumor tissues from 6 patients with head and neck cancer were collected at H. Lee Moffitt Cancer Center. The rest of the samples were collected at Helen F. Graham Cancer Center: 16 subjects with previously untreated stage III-IV non-small cell lung cancer (NSCLC), 7 patients with stage II-IV breast adenocarcinoma, 4 patients with stage III-IV colon adenocarcinoma, and 9 patients with stage III-IV head and neck squamous cells cancer. MDSC from PB were evaluated in mononuclear fraction after ficoll density gradient. The details of MDSC isolation from tumors are provided in supplemental experimental procedures. Specimens of tumor tissues and lymph nodes (without evidence of tumor cell infiltration) were obtained from Biospecimen and Pathology Core of Wistar/Upenn Melanoma SPORE.

Mice and Tumor Models

All experiments with mice were approved by University of South Florida and The Wistar Institute Animal Care and Use Committee. The mice were kept under pathogen-free conditions. C57BL/6, BALB/c, FVB/n female mice (6–8 weeks old) and CD45.1$^+$ congenic mice were obtained from NCI. HIF1$\alpha^{fl/fl}$Mx1-Cre$^{+/-}$, and STAT1 KO B6.129S(Cg)-Stat1^{tm1Dlv}/J mice were purchased from The Jackson Laboratory. STAT1 KO mice were crossed to C57BL/6 mice for 6 generations. Samples from CD45-deficient mice were obtained from Dr. Weiss, University of California, San Francisco. The doxycycline inducible c-fms-rtTA/(TetO)$_7$-CMV-Stat3C bitransgenic mice were described previously (Yan et al., 2012). For experiments with CD45-deficient mice, lethally irradiated congenic CD45.1$^+$ were reconstituted with BM cells from CD45 KO mice.

The list of tumor cells and models is provided in Supplemental Experimental Procedures. For cucurbitacin I (JSI-124; Sigma Aldrich) treatment, mice with palpable EL-4 tumors (1 week after tumor injection) were treated i.p. with 1 mg/kg/of JSI-124 for 2 weeks.

Cell Isolation and Culture

Single-cell suspensions were prepared from spleen followed by red cell removal using ammonium chloride lysis buffer. Single-cell suspensions from tumor tissues were prepared using Mouse Tumor Dissociation Kit according to the manufacturer's recommendation (Miltenyi). MDSC were purified by magnetic beads isolation using biotinylated Gr-1 antibody (Miltenyi) followed by streptavidin beads, according to the manufacturer's instructions (Miltenyi). Cells were then cultured in presence of 20% tumor explant

supernatant (TES) and 20 ng/ml recombinant GM-CSF (Invitrogen) in RPMI (Biosource International) supplemented with 10% FBS, 5 nM glutamine, 25 mM HEPES, and 1% antibiotics (Invitrogen). Hypoxia (0.5% O_2) was maintained using hypoxic chamber (BioSpherix).

Flow Cytometry and Immunofluorescence

The details of staining are provided in Supplemental Experimental Procedures.

Evaluation of pSTAT3 in MDSC in the Areas of Hypoxia in Tumor

Pimonidazole HCl, which in hypoxia forms stable covalent adducts with thiol groups of proteins, peptides, and amino acids, was used to detect hypoxia in tissue. Detection of hypoxia is based on specific antibody recognition of these adducts. 60 mg/kg pimonidazole HCl (hypoxy probe; Hypoxyprobe–1) was injected i.v. into CT-26 tumor-bearing mice. 1 hr later, tumor tissues were collected and processed for staining for cell surface markers for MDSC, followed by pSTAT3 staining.

Western Blotting

The details of are provided in Supplemental Experimental Procedures.

CD45 Tyrosine Phosphatase Activity

The CD45 PTP activity was evaluated using a colorimetric assay based on the cleavage of a synthetic phosphotyrosine peptide with the sequence of the negative regulatory site of $pp60^{c-src}$ (Enzo Life sciences).

CD45 Dimerization

Splenic MDSC from EL4 TB mice were cultured in normoxic or hypoxic condition for 36 hr. The cells were washed with PBS and incubated with 5 mM of chemical crosslinker, BS^3 (Bis[sulfosuccinimidyl] suberate) for 45 min at 37°C. The reaction was stopped by adding 20 mM Tris. The cells were washed again and whole-cells lysates were prepared and CD45 was detected under non-reducing condition by Western blot using antibody specific to CD45.

siRNA Transfection

The cells were mixed with 100 nM siRNA specific to the sequences encoding CD45 (Ambion Life Technologies) or scrambled siRNA and transfection was carried out by electroporation using an Amaxa Nucleofactor Kit (Lonza).

Electrophoretic Mobility Shift Assay

To examine the STAT3-DNA binding, we prepared nuclear extracts with either freshly isolated MDSC from spleens and tumors or splenic MDSC cultured under normoxic or hypoxic condition for 48 hr. The nuclear extracts (8 μg) were incubated with ^{32}P-labeled double-stranded STAT3 oligonucleotide (Santa Cruz Biotech) in binding buffer containing 50 μg/ml of salmon sperm DNA and BSA each. The DNA-protein complex was resolved on a non-denaturing polyacrylamide gel and analyzed by autoradiography.

Immunoprecipitation

The whole-cell lysates prepared from MDSC from the spleen and tumor of EL-4 TB mice were incubated overnight with 50 ug of agarose-bound Elderberry Bark Lectin (Vector Labs) at 4°C. The pulled-down proteins with agarose beads were separated by centrifugation, washed several times with 0.5% PBST, and boiled with sample buffer for 10 min at 99°C, followed by centrifugation at high speed to collect supernatant for the Western blot using CD45 ab to evaluate the presence of sialic acid bound to CD45.

Statistical Analyses

Statistical analyses were performed using two-tailed Student's t test and GraphPad Prism 5 software (GraphPad Software). Paired t test was used most of the time because data were normally distributed. All the data are presented as mean ± SEM and p value less than 0.05 was considered significant. The repeated-measurements of tumor growth kinetic were assessed in two-way ANOVA test.

Supplementary Material

Refer to Web version on PubMed Central for supplementary material.

Acknowledgments

References

Abad C, Nobuta H, Li J, Kasai A, Yong WH, Waschek JA. Targeted STAT3 disruption in myeloid cells alters immunosuppressor cell abundance in a murine model of spontaneous medulloblastoma. J Leukoc Biol. 2014; 95:357–367. [PubMed: 24068730]

Bain CC, Bravo-Blas A, Scott CL, Gomez Perdiguero E, Geissmann F, Henri S, Malissen B, Osborne LC, Artis D, Mowat AM. Constant replenishment from circulating monocytes maintains the macrophage pool in the intestine of adult mice. Nat Immunol. 2014; 15:929–937. [PubMed: 25151491]

Bharadwaj U, Li M, Zhang R, Chen C, Yao Q. Elevated inter-leukin-6 and G-CSFin human pancreatic cancer cell conditioned medium suppress dendritic cell differentiation and activation. Cancer Res. 2007; 67:5479–5488. [PubMed: 17545630]

Blaskovich MA, Sun J, Cantor A, Turkson J, Jove R, Sebti SM. Discovery of JSI-124 (cucurbitacin I), a selective Janus kinase/signal transducer and activator of transcription 3 signaling pathway inhibitor with potent antitumor activity against human and murine cancer cells in mice. Cancer Res. 2003; 63:1270–1279. [PubMed: 12649187]

Corzo CA, Condamine T, Lu L, Cotter MJ, Youn JI, Cheng P, Cho HI, Celis E, Quiceno DG, Padhya T, et al. HIF-1α regulates function and differentiation of myeloid-derived suppressor cells in the tumor micro-environment. J Exp Med. 2010; 207:2439–2453. [PubMed: 20876310]

Doedens AL, Stockmann C, Rubinstein MP, Liao D, Zhang N, DeNardo DG, Coussens LM, Karin M, Goldrath AW, Johnson RS. Macrophage expression of hypoxia-inducible factor-1 alpha suppresses T-cell function and promotes tumor progression. Cancer Res. 2010; 70:7465–7475. [PubMed: 20841473]

Franklin RA, Liao W, Sarkar A, Kim MV, Bivona MR, Liu K, Pamer EG, Li MO. The cellular and molecular origin of tumor-associated macrophages. Science. 2014; 344:921–925. [PubMed: 24812208]

Gabrilovich DI, Nagaraj S. Myeloid-derived suppressor cells as regulators of the immune system. Nat Rev Immunol. 2009; 9:162–174. [PubMed: 19197294]

Gabrilovich DI, Ostrand-Rosenberg S, Bronte V. Coordinated regulation of myeloid cells by tumours. Nat Rev Immunol. 2012; 12:253–268. [PubMed: 22437938]

Galdiero MR, Garlanda C, Jaillon S, Marone G, Mantovani A. Tumor associated macrophages and neutrophils in tumor progression. J Cell Physiol. 2013; 228:1404–1412. [PubMed: 23065796]

Hasita H, Komohara Y, Okabe H, Masuda T, Ohnishi K, Lei XF, Beppu T, Baba H, Takeya M. Significance of alternatively activated macrophages in patients with intrahepatic cholangiocarcinoma. Cancer Sci. 2010; 101:1913–1919. [PubMed: 20545696]

Herrmann A, Kortylewski M, Kujawski M, Zhang C, Reckamp K, Armstrong B, Wang L, Kowolik C, Deng J, Figlin R, Yu H. Targeting Stat3 in the myeloid compartment drastically improves the in vivo antitumor functions of adoptively transferred T cells. Cancer Res. 2010; 70:7455–7464. [PubMed: 20841481]

Holmes N. CD45 : all is not yet crystal clear. Immunology. 2006; 117:145–155. [PubMed: 16423050]

Kaplan-Lefko PJ, Chen TM, Ittmann MM, Barrios RJ, Ayala GE, Huss WJ, Maddison LA, Foster BA, Greenberg NM. Pathobiology of autochthonous prostate cancer in a pre-clinical transgenic mouse model. Prostate. 2003; 55:219–237. [PubMed: 12692788]

Kato M, Takahashi M, Akhand AA, Liu W, Dai Y, Shimizu S, Iwamoto T, Suzuki H, Nakashima I. Transgenic mouse model for skin malignant melanoma. Oncogene. 1998; 17:1885–1888. [PubMed: 9778055]

Ko JS, Rayman P, Ireland J, Swaidani S, Li G, Bunting KD, Rini B, Finke JH, Cohen PA. Direct and differential suppression of myeloid-derived suppressor cell subsets by sunitinib is compartmentally constrained. Cancer Res. 2010; 70:3526–3536. [PubMed: 20406969]

Komohara Y, Ohnishi K, Kuratsu J, Takeya M. Possible involvement of the M2 anti-inflammatory macrophage phenotype in growth of human gliomas. J Pathol. 2008; 216:15–24. [PubMed: 18553315]

Kortylewski M, Kujawski M, Wang T, Wei S, Zhang S, Pilon-Thomas S, Niu G, Kay H, Mulé J, Kerr WG, et al. Inhibiting Stat3 signaling in the hematopoietic system elicits multicomponent antitumor immunity. Nat Med. 2005; 11:1314–1321. [PubMed: 16288283]

Kujawski M, Kortylewski M, Lee H, Herrmann A, Kay H, Yu H. Stat3 mediates myeloid cell-dependent tumor angiogenesis in mice. J Clin Invest. 2008; 118:3367–3377. [PubMed: 18776941]

Meyer C, Sevko A, Ramacher M, Bazhin AV, Falk CS, Osen W, Borrello I, Kato M, Schadendorf D, Baniyash M, Umansky V. Chronic inflammation promotes myeloid-derived suppressor cell activation blocking antitumor immunity in transgenic mouse melanoma model. Proc Natl Acad Sci USA. 2011; 108:17111–17116. [PubMed: 21969559]

Nefedova Y, Huang M, Kusmartsev S, Bhattacharya R, Cheng P, Salup R, Jove R, Gabrilovich D. Hyperactivation of STAT3 is involved in abnormal differentiation of dendritic cells in cancer. J Immunol. 2004; 172:464–474. [PubMed: 14688356]

Nefedova Y, Cheng P, Gilkes D, Blaskovich M, Beg AA, Sebti SM, Gabrilovich DI. Activation of dendritic cells via inhibition of Jak2/STAT3 signaling. J Immunol. 2005a; 175:4338–4346. [PubMed: 16177074]

Nefedova Y, Nagaraj S, Rosenbauer A, Muro-Cacho C, Sebti SM, Gabrilovich DI. Regulation of dendritic cell differentiation and anti-tumor immune response in cancer by pharmacologic-selective inhibition of the janus-activated kinase 2/signal transducers and activators of transcription 3 pathway. Cancer Res. 2005b; 65:9525–9535. [PubMed: 16230418]

Noy R, Pollard JW. Tumor-associated macrophages: from mechanisms to therapy. Immunity. 2014; 41:49–61. [PubMed: 25035953]

Park SJ, Nakagawa T, Kitamura H, Atsumi T, Kamon H, Sawa S, Kamimura D, Ueda N, Iwakura Y, Ishihara K, et al. IL-6 regulates in vivo dendritic cell differentiation through STAT3 activation. J Immunol. 2004; 173:3844–3854. [PubMed: 15356132]

Rébé C, Végran F, Berger H, Ghiringhelli F. STAT3 activation: A key factor in tumor immunoescape. JAK-STAT. 2013; 2:e23010. [PubMed: 24058791]

Schulz C, Gomez Perdiguero E, Chorro L, Szabo-Rogers H, Cagnard N, Kierdorf K, Prinz M, Wu B, Jacobsen SE, Pollard JW, et al. A lineage of myeloid cells independent of Myb and hematopoietic stem cells. Science. 2012; 336:86–90. [PubMed: 22442384]

Shand FH, Ueha S, Otsuji M, Koid SS, Shichino S, Tsukui T, Kosugi-Kanaya M, Abe J, Tomura M, Ziogas J, Matsushima K. Tracking of intertissue migration reveals the origins of tumor-infiltrating monocytes. Proc Natl Acad Sci USA. 2014; 111:7771–7776. [PubMed: 24825888]

Shim SH, Sung MW, Park SW, Heo DS. Absence of STAT1 disturbs the anticancer effect induced by STAT3 inhibition in head and neck carcinoma cell lines. Int J Mol Med. 2009; 23:805–810. [PubMed: 19424608]

Solito S, Bronte V, Mandruzzato S. Antigen specificity of immune suppression by myeloid-derived suppressor cells. J Leukoc Biol. 2010; 90:31–36. [PubMed: 21486906]

Stark GR, Darnell JE Jr. The JAK-STAT pathway at twenty. Immunity. 2012; 36:503–514. [PubMed: 22520844]

Sun Z, Yao Z, Liu S, Tang H, Yan X. An oligonucleotide decoy for Stat3 activates the immune response of macrophages to breast cancer. Immunobiology. 2006; 211:199–209. [PubMed: 16530087]

Trikha P, Carson WE 3rd. Signaling pathways involved in MDSC regulation. Biochim Biophys Acta. 2014; 1846:55–65. [PubMed: 24727385]

Tu SP, Jin H, Shi JD, Zhu LM, Suo Y, Lu G, Liu A, Wang TC, Yang CS. Curcumin induces the differentiation of myeloid-derived suppressor cells and inhibits their interaction with cancer cells and related tumor growth. Cancer Prev Res (Phila). 2012; 5:205–215. [PubMed: 22030090]

Vasquez-Dunddel D, Pan F, Zeng Q, Gorbounov M, Albesiano E, Fu J, Blosser RL, Tam AJ, Bruno T, Zhang H, et al. STAT3 regulates arginase-I in myeloid-derived suppressor cells from cancer patients. J Clin Invest. 2013; 123:1580–1589. [PubMed: 23454751]

Wu L, Bijian K, Shen SH. CD45 recruits adapter protein DOK-1 and negatively regulates JAK-STAT signaling in hematopoietic cells. Mol Immunol. 2009; 46:2167–2177. [PubMed: 19481264]

Xin H, Zhang C, Herrmann A, Du Y, Figlin R, Yu H. Sunitinib inhibition of Stat3 induces renal cell carcinoma tumor cell apoptosis and reduces immunosuppressive cells. Cancer Res. 2009; 69:2506–2513. [PubMed: 19244102]

Xu Z, Weiss A. Negative regulation of CD45 by differential homo-dimerization of the alternatively spliced isoforms. Nat Immunol. 2002; 3:764–771. [PubMed: 12134145]

Yan C, Qu P, Du H. Myeloid-specific expression of Stat3C results in conversion of bone marrow mesenchymal stem cells into alveolar type II epithelial cells in the lung. Sci China Life Sci. 2012; 55:576–590. [PubMed: 22864832]

Yin J, Hashimoto A, Izawa M, Miyazaki K, Chen GY, Takematsu H, Kozutsumi Y, Suzuki A, Furuhata K, Cheng FL, et al. Hypoxic culture induces expression of sialin, a sialic acid transporter, and cancer-associated gangliosides containing non-human sialic acid on human cancer cells. Cancer Res. 2006; 66:2937–2945. [PubMed: 16540641]

Yu H, Lee H, Herrmann A, Buettner R, Jove R. Revisiting STAT3 signalling in cancer: new and unexpected biological functions. Nat Rev Cancer. 2014; 14:736–746. [PubMed: 25342631]

Highlights

- MDSC differentiation to TAM in hypoxic environment is regulated by STAT3 activity

- STAT3 inhibition in MDSC was caused by upregulation of CD45 phosphatase activity

- Activation of CD45 phosphatase was mediated by sialic acid

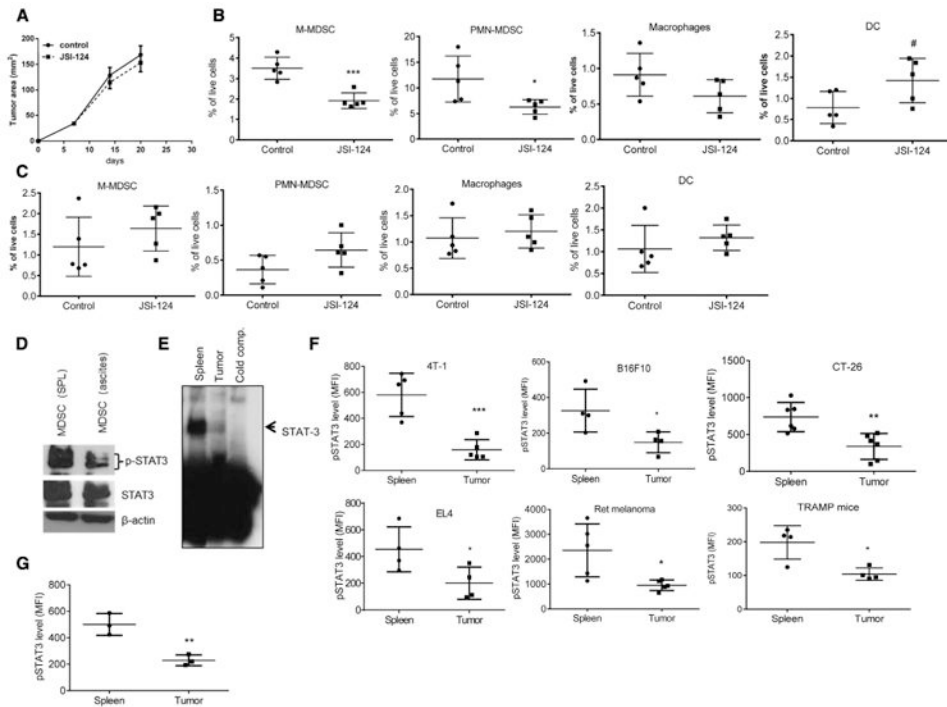- Degradation of sialic acid sensitized tumor myeloid cells to STAT3 inhibitor

Figure 1. Downregulation of STAT3 Activity in Tumor MDSC

(A–C) EL4 TB mice were treated with 1 mg/kg JSI-124 or vehicle control for 2 weeks and the kinetics of tumor growth (A) as well as the proportions of cells in spleens (B) and tumors (C) were evaluated (n = 3). *$p < 0.05$; ***$p < 0.001$; #$p < 0.05$ in one-tailed t test.

(D) Phospho-tyrosine pSTAT3 in MDSC isolated from spleens and tumor site (ascites). The experiments were performed three times with the same results.

(E). STAT3-DNA binding in MDSC from spleen and tumor measured by EMSA. Two experiments with the similar results were performed. Cold competition–50× unlabeled probe added to spleen MDSC sample.

(F). Mean fluorescence intensity (MFI) of intracellular pSTAT3 staining in MDSC isolated from spleens and s.c. tumors (as indicated). Spleen and tumor cells were subjected to enzymatic digestion as described in methods. Each group included four mice. *$p < 0.05$, **$p < 0.01$, ***$p < 0.001$.

(G) pSTAT3 expression in CD11b$^+$Gr-1$^-$F4/80$^+$ macrophages from tumor and spleens of CT-26 TB mice. Each group included three mice. **$p < 0.01$.
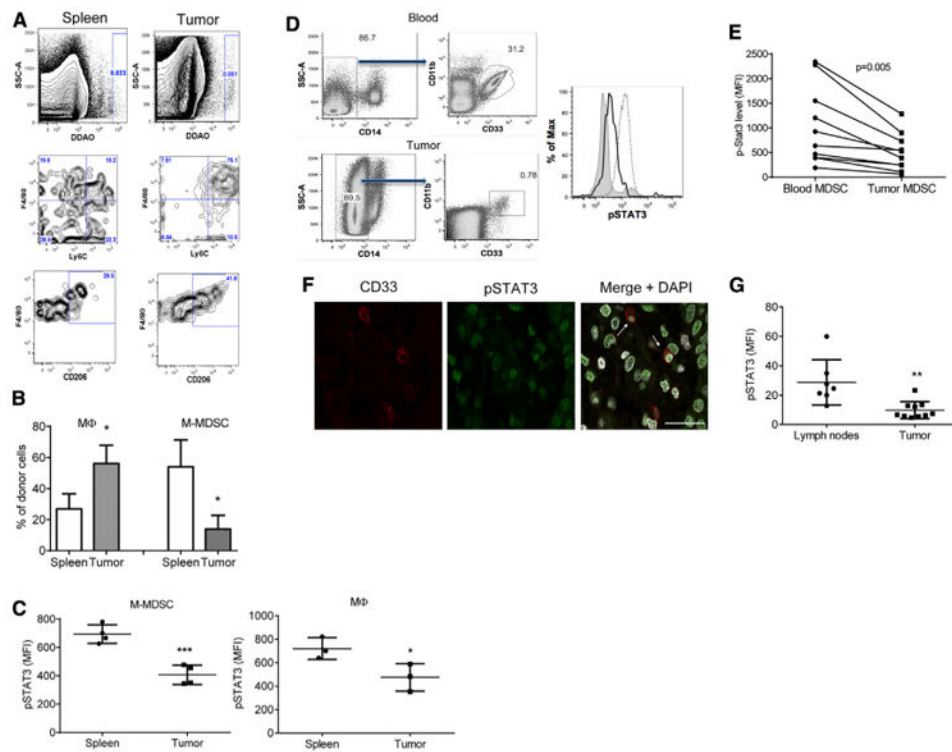
Figure 2. STAT3 Regulates the Fate of MDSC in Tumor Site

(A–C) CD11b$^+$Ly6C^{hi}Ly6G$^-$F4/80$^-$ M-MDSC were sorted from BM of EL-4 TB mice, labeled with fluorescent dye DDAO and 5×10^6 cells were injected i.v into s.c. EL-4 TB recipients. Cells in spleens and tumors were evaluated by flow cytometry 48 hr after the transfer. (A) A typical example of the analysis. (B) The proportion of M-MDSC and macrophages among DDAO positive donor's cells. Each group included 3 mice. **p < 0.01 between spleen and tumor. (C) Intracellular pSTAT3 within the population of donor's M-MDSC and macrophages in spleen and tumors. Intensity of fluorescence is shown. *p < 0.05 between groups.

(D) A typical example of the gating strategy of MDSC from peripheral blood and tumor tissues of the HNC patients (left) and pSTAT3 level (right) analyzed by flow cytometry. (Solid line-tumor MDSC, dotted line-MDSC from spleen, gray filled histogram-isotype control.)

(E) The cumulative results of ten patients examined.

(F and G) pSTAT3 in myeloid cells in melanoma tissues and uninvolved (tumor-free) lymph nodes from the same patient. (F) Atypical example of staining of CD33$^+$ myeloid cells (pointed by arrows). Scale bar represents 25 μm. (G) Intensity of fluorescence of pSTAT3 in nuclei of CD33$^+$ myeloid cells. **p < 0.01.
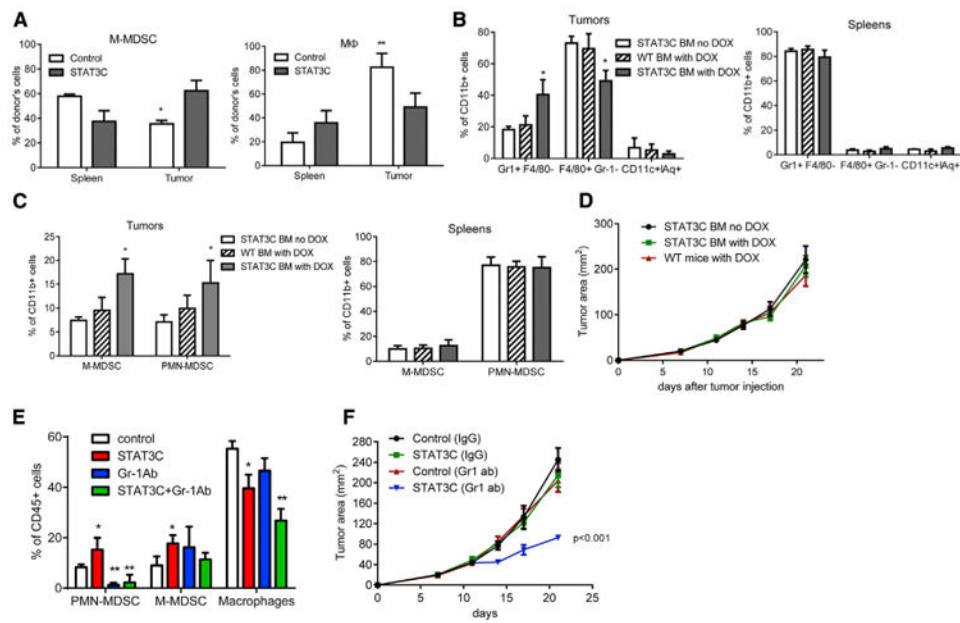
Figure 3. Effect of Constitutive Expression of STAT3C on Myeloid Cell Differentiation in Tumor Site

(A–D) Lethally irradiated FVB/n recipients were reconstituted with BM from STAT3C mice and treated with doxycycline to induce STAT3 activation. Eight weeks after BM transfer, mice were injected s.c. with syngeneic ANV tumor cells. (A) 3 weeks later, BM M-MDSC were sorted, labeled with DDAO, and transferred to ANV TB recipients. DDAO positive donor's myeloid cells in spleens and tumors were evaluated 48 hr after the transfer. Each group included three mice. *p < 0.05; **p <0.01 between spleen and tumor. (B) Populations ofCD11b$^+$ myeloid cells in tumors and spleens evaluated 3 weeks after tumor injection (n = 5). (C) M-MDSC and PMN-MDSC in tumors and spleens (n = 5).*p < 0.05 from no-doxycycline control. (D) The kinetics of the tumor growth in mice. Each group included five mice. (E and F) Recipients of STAT3C or control BM were treated with 250 μg of Gr-1 ab i.p. or control IgG twice a week for 2 weeks starting 1 week after tumor inoculation. (E) The phenotype of myeloid cells in tumors. *p < 0.05, **p < 0.01 from control (n = 4); (F) Tumor growth kinetics showing the tumor area (mm^2) of control and STAT3C TB mice treated with or without Gr-1 ab. Each group included four mice. p values difference from control group calculated in two-way ANOVA test.
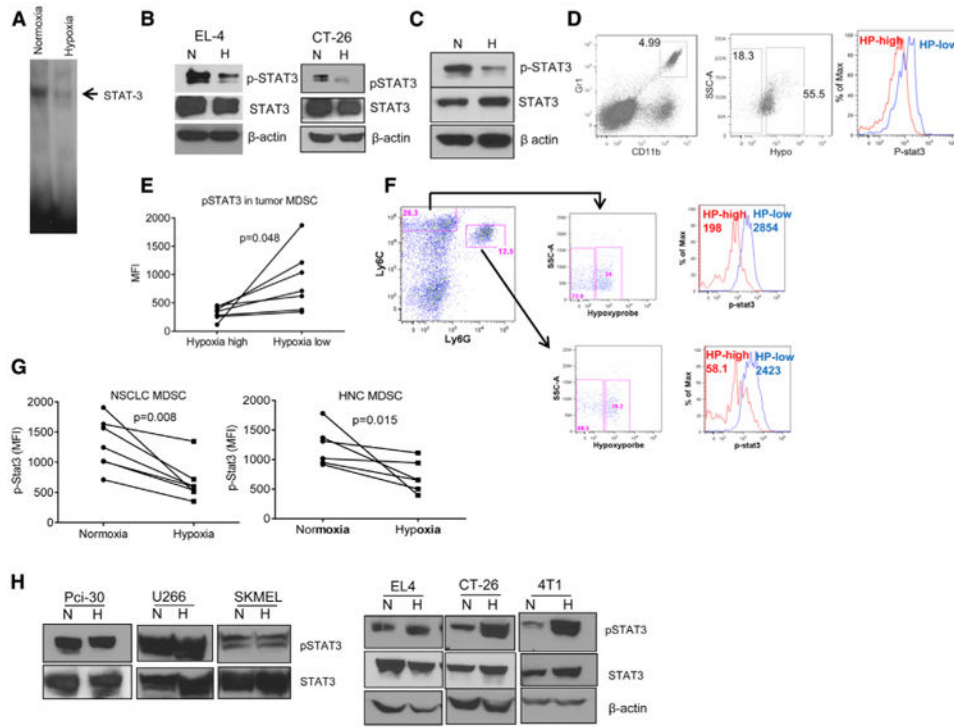
Figure 4. Hypoxia Inhibits STAT3 Activity in Myeloid Cells

(A) STAT3 EMSA with the nuclear proteins prepared from MDSC from spleen of EL4 TB mice cultured with 20 ng/ml GM-CSF and 20% TES in normoxia or hypoxia for 48 hr. Two experiments with the same results were performed.

(B) Gr-1 $^+$CD11b$^+$ MDSC from spleens of EL4 or CT-26 TB mice were cultured in normoxia or hypoxia for 48 hr as described above and pSTAT3 was evaluated by Western blot. Six experiments with the same results were performed.

(C) M-MDSC from spleen of EL4 TB mice were treated and evaluated as described in Figure 4B.

(D) A typical example of gating of Gr-1 $^+$CD11b$^+$ MDSC from tumor of CT-26 TB mice (left panel). MDSC were further gated based on the intensity of hypoxyprobe staining (middle panel) and pSTAT3 was evaluated in cells stained with hypoxyprobe (right panel). (HP-high-hypoxyprobe staining high-red color, HP-low-hypoxyprobe staining low-blue color.)

(E) Cumulative results of seven experiments performed.

(F) Experiment was performed as described in Figure 4D. PMN-MDSC and M-MDSC were gated based on the intensity of hypoxyprobe staining.

(G) Mononuclear fractions were isolated from peripheral blood of NSCLC and HNC patients and cultured with GM-CSF and 20% TCM from SKMEL tumor cells in normoxia or hypoxia for 48 hr. pSTAT3 level was examined in CD11b$^+$CD14$^-$CD33$^+$ MDSC by flow cytometry.

(H) pSTAT3 in human (left panel panels) and mouse (right panels) tumor cells lines cultured in normoxic/hypoxic condition evaluated by Western blot.
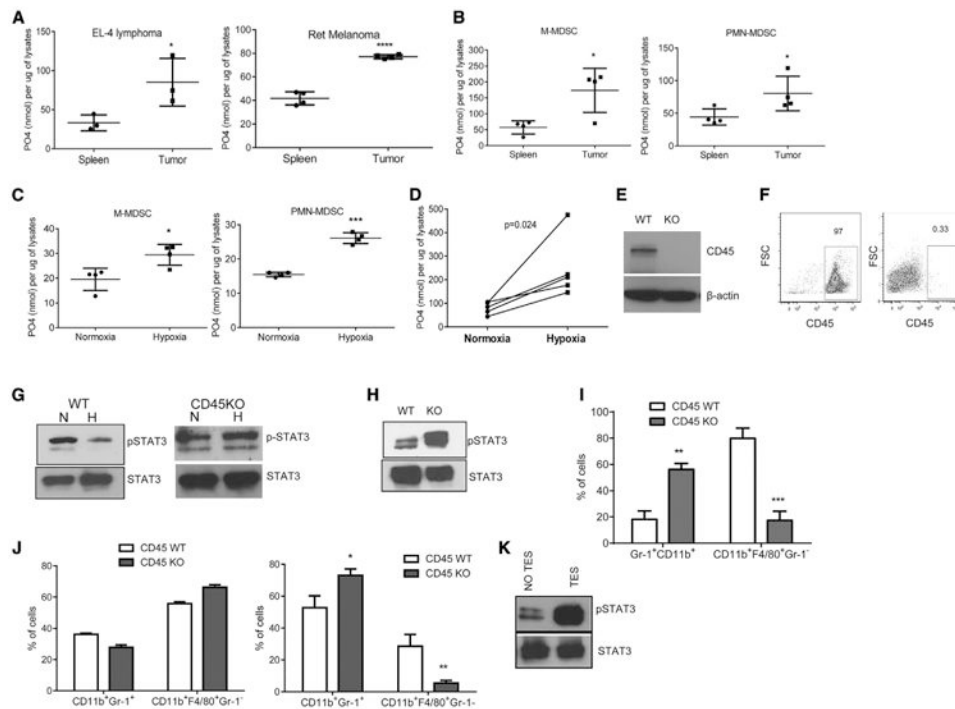
Figure 5. Hypoxia Upregulates CD45 PTP Activity in Myeloid Cells

(A) CD45PTP activity (nmol of PO_4 released per μg of lysates) in Gr-1$^+$CD11b$^+$ MDSC from spleen and tumors of the same EL4 TB mice (n = 3) or Ret TB mice (n = 4).

(B) The same experiments performed with M-MDSC and PMN-MDSC isolated from spleens and tumors of EL4 TB mice (n = 4).

(C) Splenic M-MDSC and PMN-MDSC cultured in normoxic/hypoxic conditions with GM-CSF and TES for 48 hr (n = 4). *p < 0.05, ***p < 0.001.

(D) CD45PTP activity in MDSC isolated from PB of HNC patients cultured in hypoxia for 36 hr with GM-CSF and TCM;

(E and F) CD45 expression in WT and CD45 KO BM cells detected by Western blot (E) and flow cytometry (F).

(G) Enriched HPC from WT or CD45KO mice were cultured for 6 days with 20 ng/ml GM-CSF and 20% TES. Gr-1$^+$CD11b$^+$ cells were purified and cultured in hypoxia for 48 hr. pSTAT3 was detected in Western blot. Experiments were performed twice with the same results.

(H) pSTAT3 in Gr-1$^+$CD11b$^+$ cells generated from HPC isolated from WT or CD45 KO mice. Two experiments with the same results were performed.

(I) Enriched HPC from WT or CD45KO mice were cultured for 6 days with 20% TES in the presence of GM-CSF. Gr-1$^+$CD11b$^+$ MDSC were purified and labeled with CMFDA and DDAO respectively and injected directly to ascites of EL4 TB mice. CMFDA/DDAO positive cells recovered 48 hr later from the ascites were evaluated by flow cytometry. Three mice per group were used. **p < 0.001.

(J) Enriched HPC from WT or CD45KO mice were cultured for 6 days either without (left panel) or with (right panel) 20% TES in the presence of GM-CSF. The phenotype of

myeloid cells was evaluated by flow cytometry. Each group included three mice. *$p < 0.05$; **$p < 0.01$.

(K) pSTAT3 in Gr-1$^+$CD11b$^+$ cells generated from HPC with GM-CSF in the presence or absence of TES. Two experiments with the same results were performed.
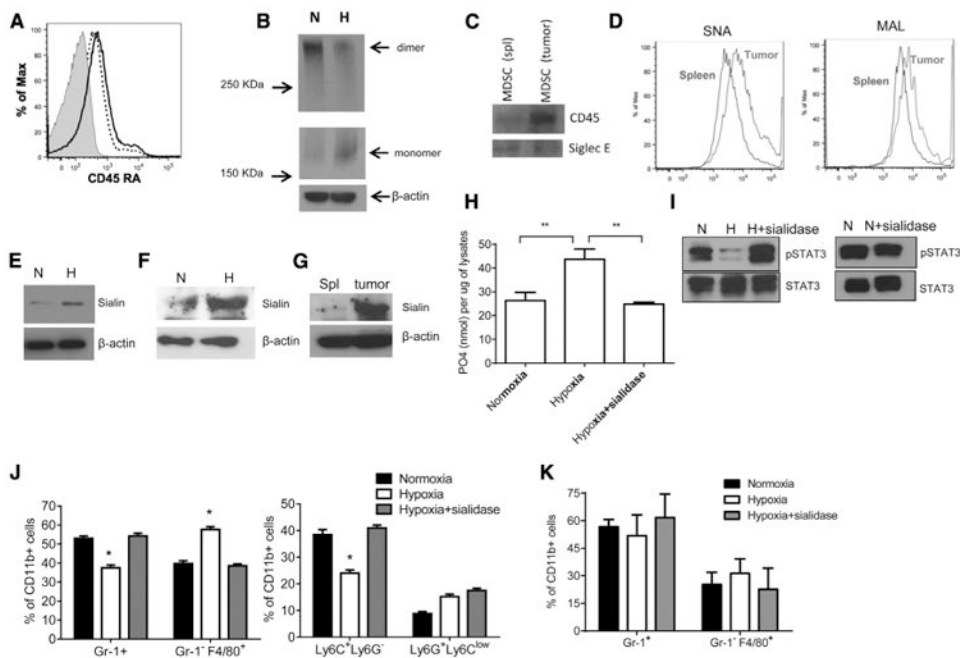
Figure 6. The Mechanism of CD45 Activation in Hypoxia

(A) CD45 RA expression on the surface of MDSC from spleens of EL4 TB mice cultured in normoxic (dotted line) or hypoxic (solid line) condition for 36 hr with TES and GM-CSF.

(B) MDSC from spleen of EL4 TB mice were cultured in normoxic or hypoxic condition for 36 hr, followed by crosslink and detection of CD45 under non-reducing condition by Western blot. Two experiments with the same results were performed.

(C) Binding of SA to CD45 in spleen and tumor MDSC. SA was pulled down using agarose bound lectin and membranes were probed with CD45 ab. Siglec E ab was used as loading control. Five experiments with the similar results were performed.

(D) SA on the surface of MDSC sorted from spleen (blue line) and tumor (red line) of EL4 TB mice and incubated with FITC-labeled SNA lectin (left panel) or biotinylated MAL lectin, followed by streptavidin-FITC (right panel). Typical example of three performed experiments is shown.

(E and F) Sialin in MDSC from spleens (E) of EL4 TB mice or PB of HNC patients (F) cultured under normoxic/hypoxic condition for 48 hr in the presence of TES/TCM and GM-CSF.

(G) The amount of sialin in MDSC isolated from spleens and tumors of the same EL4 TB mice. Three experiments with the similar results were performed.

(H and I) MDSC from spleens of EL4 TB mice were treated with 0.05 U/ml sialidase or left untreated and cultured in normoxic/hypoxic condition for 36 hr with TES and GM-CSF. CD45 PTP activity (H) and pSTAT3 (I) were evaluated. Data are representative of three experiments.

(J and K) Enriched HPC from BM of naive (J) or STAT3C (K) mice were cultured with 20 ng/ml GM-CSF and 20% TES. Cells were exposed to hypoxia from day 2 and incubated for 4 more days. 0.05 U/ml sialidase was used. The proportion of myeloid cells was evaluated by flow cytometry (n = 3). $*p < 0.05$.
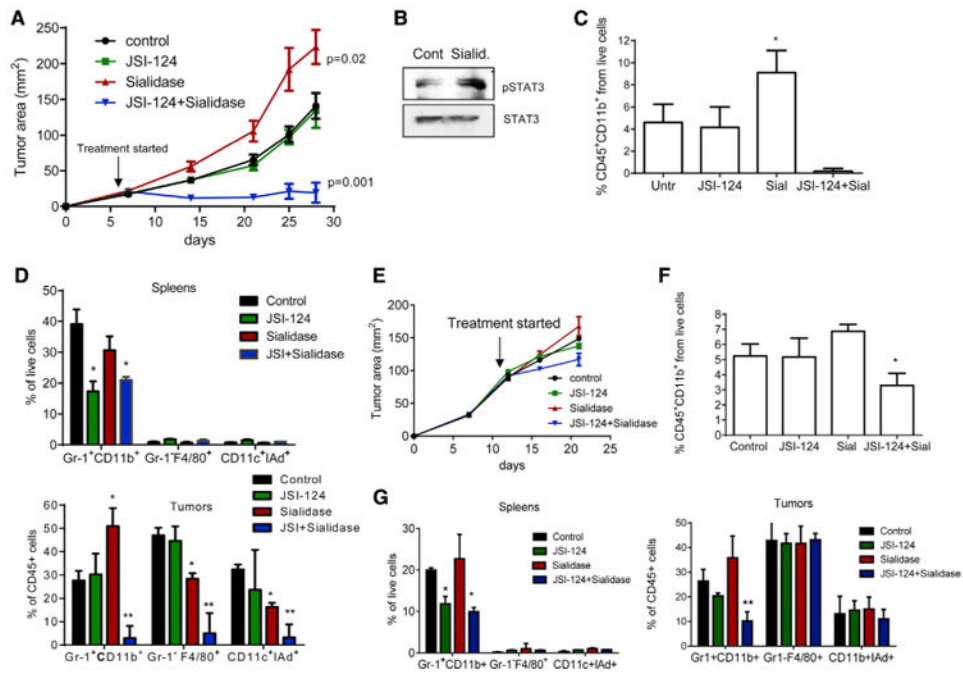
Figure 7. Targeting of CD45PTP Activation Sensitizes Tumor Myeloid Cells to STAT3 Inhibitor

(A–D) MethA sarcoma cells (0.5×10^6) were injected s.c. into BALB/c mice. 7 days later mice were treated with JSI-124 (1 mg/kg i.p. daily for 6 days per week for 3 weeks) alone or in combination with sialidase (intratumoral administration, twice a week, 200 mU/mouse for 3 weeks). (A) Tumor size. Each group included 6 mice. p values calculated in two-way ANOVA from control group. (B) pSTAT3 in Gr-1$^+$CD11b$^+$ cells isolated from tumors of mice treated with sialidase alone. Two experiments with the same results were performed. (C) The proportion of CD45$^+$CD11b$^+$ myeloid cells in total population of live cells in tumors (n = 4). *p < 0.05 from control. (D) Populations of spleen and tumor myeloid cells in MethA sarcoma bearing mice treated as described above. *p < 0.05; **p < 0.01 from untreated control.

(E–G) MethA sarcoma TB mice were treated from day 14 days after tumor inoculation with the same way as in Figures 7A–7D with exception of duration of treatment. JSI-124 was administrated for only 10 days and sialidase only three times. (E) Tumor size (4 mice per group). (F) The proportion of CD45$^+$CD11b$^+$ myeloid cells in total population of live cells in tumors (n = 4). *p < 0.05 from control. (G) Populations of spleen and tumor myeloid cells in mice treated as described above. *p < 0.05; **p < 0.01 from untreated control.